Biochemistry

 Volume 32, Number 20 May 25, 1993

Articles

Multiple Magnesium Ions in the Ribonuclease P Reaction Mechanism†

Drew Smith‡ and Norman R. Pace*

Department of Biology and Institute for Molecular and Cellular Biology, Indiana University, Bloomington, Indiana 47405

Received September 28, 1992; Revised Manuscript Received March 4, 1993

ABSTRACT: The ribozyme ribonuclease (RNase) P cleaves precursor transcripts to produce the mature 5′-end of tRNAs. This hydrolysis reaction has a divalent cation requirement that is primarily catalytic, rather than structural; RNase P can be considered a metalloenzyme. Kinetic analysis shows that the RNase P catalytic mechanism has a cooperative dependence upon Mg^{2+} concentration. At least three Mg^{2+} ions are required for optimal activity, suggesting a multiple metal ion mechanism. The 2′-OH at the site of substrate cleavage may act as a ligand for a catalytically important Mg^{2+}: deoxyribose substitution reduces the apparent number of Mg^{2+} bound from three to two and increases the apparent dissociation constant for Mg^{2+} from the micromolar to the millimolar range. In addition to these cation effects, the deoxyribose substitution reduces the rate of catalysis by 3400-fold; substitution with 2′-*O*-methyl at the cleavage site reduces the catalytic rate 10^6-fold. If we presume no significant conformational effects of the substitutions, these results suggest that the 2′-OH serves as hydrogen-bond donor. The kinetic analysis of the catalytic mechanism is based upon the characterization of the pH dependence of the reaction. There is a hyperbolic (saturable) dependence on hydroxide concentration, with the half-maximal rate achieved at pH 8.0–8.5. The rate of the cleavage step is about 200 min^{-1} at pH 8.0, which is 500-fold faster than the steady-state parameter k_{cat}.

Ribonuclease (RNase) P, which is found in all organisms, generates the mature 5′-end of tRNAs by endonucleolytic cleavage of precursor transcripts. In eubacteria the enzyme is a ribonucleoprotein composed of a small (ca. 14 kDa) protein subunit and a catalytic RNA (ca. 140 kDa) [reviewed by Brown and Pace, (1992)]. Under the appropriate ionic conditions in vitro, the RNA can act without the protein [reviewed by Pace and Smith (1990)]. Although the cleavage reaction requires a divalent cation, RNase P RNA is able to bind its substrate, pre-tRNA, without any divalent cations (Smith et al., 1992), indicating that the divalent cation requirement is for catalysis, rather than structure. Because the action of Mg^{2+} is likely to be central to catalysis by RNase P (and other ribozymes), we have made a more detailed study of its role and its interaction with other components of the reaction mechanism.

The RNase P hydrolysis reaction may be written as

$$E + S \underset{k_{-1}}{\overset{k_1}{\rightleftharpoons}} E{\cdot}S \xrightarrow{k_2} E{\cdot}P \underset{k_{-3}}{\overset{k_3}{\rightleftharpoons}} E + P \qquad (1)$$

where E is the RNase P, S is the pre-tRNA, and P is the mature tRNA. Under steady-state conditions, product release is the rate-limiting step of the reaction (Reich et al., 1988); consequently, the steady-state Michaelian parameters are uninformative with respect to k_2, the chemical step of the reaction. Using pre-steady-state analysis of slow reactions, we developed a scheme to evaluate k_2. We studied the contributions of several reaction components to catalysis: the substrate phosphodiester linkage, divalent cation, and the hydrolytic water. This analysis indicates the following: (1)

† D.S. was the recipient of postdoctoral fellowships from the Indiana Institute for Molecular and Cellular Biology and the National Institutes of Health (GM13712). N.P. was the recipient of National Institutes of Health Research Grant GM34537.

* Corresponding author: Telephone (812) 855-6152, FAX (812) 855-6705.

‡ Current address: NeXagen, Inc., 2860 Wilderness Pl., Boulder, CO 80301.

0006-2960/93/0432-5273$04.00/0

the 2′-OH of the cleaved phosphodiester linkage contributes a 3400-fold rate enhancement to catalysis; (2) at least three Mg^{2+} ions are bound to the E·S complex; and (3) the 2′-OH group of the cleaved phosphodiester may be a ligand to Mg^{2+}.

MATERIALS AND METHODS

RNAs. We produced RNAs by in vitro run-off transcription using bacteriophage T7 RNA polymerase (purified by Bernadette Pace) under the conditions described by Milligan and Uhlenbeck (1989). Uniform labeling was accomplished by the inclusion of 50–100 μCi of [α-^{32}P]GTP (3000 Ci/mmol, Amersham) in the transcription reactions. *Escherichia coli* RNase P RNA was transcribed from pDW98 linearized with *Bst*NI; substrates were transcribed for plasmids DW153 (*Bacillus subtilis* pre-tRNA^{Asp}) and 67YF0 (*Saccharomyces cerevisiae* tRNA^{Phe}), described in Burgin et al. (1990). RNA concentrations were determined by the specific activities of labeled RNAs or by absorbance at 260 nm.

Preparation of Modified tRNAs. Pre-tRNAs having a single nucleotide leader were produced by initiating transcription of the mature yeast tRNA^{Phe} gene with dinucleotides. The dinucleotides used were adenylylguanosine (rApG; a gift from R. I. Gumport, University of Illinois), deoxyadenylylguanosine (dApG), and 2′-*O*-methyladenylylguanosine (rAmpG). The latter two dinucleotides were synthesized by L. Washington on an ABS 360A DNA synthesizer, using phosphoramidites and columns supplied by Glenn Research. After deprotection, these dinucleotides were isolated by descending chromatography on Whatman 3MM paper in 50% EtOH/0.5 M NH_4OAc; they were eluted from the paper in water, dried, and resuspended in water three times.

Dinucleotides were analyzed by base hydrolysis in 10% piperidine at 90 °C for 1 h, followed by thin-layer chromatography on poly(ethylenimine) (PEI) cellulose in 1 M LiCl. As expected, rApG was hydrolyzed to Ap and G_{OH}, while no degradation of dApG or rAmpG was observed. The dinucleotides were also digested with nuclease P1, and their identities were confirmed by thin-layer chromatography of the digestion products on PEI cellulose in 1.2 M LiCl/1.2% boric acid. This system resolves dA_{OH} from rA_{OH} (Randerath & Randerath, 1967). The identity of the rAmpG dinucleotide was confirmed by thin-layer chromatography of the digestion products on cellulose in isopropyl alcohol/HCl and also in butyric acid/NH_4OH, which resolves 2′-*O*-methyladenosine from adenosine (Randerath & Randerath, 1967).

Incorporation of the dinucleotides dApG and rAmpG into the pre-tRNA transcript was confirmed by piperidine hydrolysis of the uniformly labeled transcripts followed by thin-layer chromatography on PEI cellulose in 1 M LiCl, which resolves the base-resistant dinucleotides (dApG and rAmpG) from 3′-mononucleoside phosphates and pppGp. Experiments with various ratios of dApG to GTP indicated that the dinucleotide was incorporated in approximate proportion to the dAPG:GTP ratio.

Transcription reactions routinely used a 6:1 ratio of dinucleotide to GTP. A small amount (1 μCi) of [α-^{32}P]GTP was included to permit quantitation of transcripts. After gel purification, the pre-tRNAs were 5′-end-labeled using polynucleotide kinase and [γ-^{32}P]ATP (Amersham, 6000 Ci/mmol) diluted to 2×10^6 dpm/pmol with unlabeled ATP. The efficiency of incorporation, and hence the specific activity of the pre-tRNA, was monitored by thin-layer chromatography on PEI cellulose in 0.75 M KH_2PO_4, pH 3.5. Typically, 40–60% of the pre-tRNAs initiated with dA and rA were labeled; incorporation of the rAm-initiated pre-tRNA was 20–40%. Unincorporated ATP was separated from the pre-tRNA by elution over a 0.2-mL Sephadex G-50 spin column, followed by precipitation in 0.3 M NaOAc (pH 5) and 2.5 vol of EtOH. Each of these steps removes approximately 90% of the free nucleotide.

Cross-Linking. Cross-linking reactions were performed essentially as described (Smith et al., 1992) in a standard reaction mix: 100 nM *E. coli* RNase P RNA, 50 nM azidophenacyl-tRNA^{Phe}, 1.0 M NaCl, 25 mM $MgCl_2$, 50 mM Tris-HCl (pH 8), and 0.05% Nonidet P-40. All components of the reactions were mixed in a microcentrifuged tube and allowed to equilibrate in the dark for 2–5 min. Open tubes were exposed to 302-nm light at room temperature for 15 min.

pH was controlled by buffering with 16.5 mM PIPES/44 mM Tris (PT buffer) in order to maintain constant ionic strength and buffering capacity over the range of measurements made (Ellis & Morrison, 1982). Stock solutions (20×) were titrated to the appropriate pH with HCl or NaOH at 37 °C. Although NH_4^+ is commonly used as the monovalent cation in RNase P reactions, it is inappropriate for use in pH studies because it is a weak acid with a pK_a of 9.3; we used Na^+ instead.

Kinetic analyses of the cleavage reaction were performed in 1.0 M NaCl, 25 mM $MgCl_2$, 0.05% Nonidet P-40, 16.5 mM PIPES, and 44 mM Tris (pH 8.0) at 37 °C, with alterations as noted. Enzymes and substrates were equilibrated separately in the reaction buffer at the reaction temperature for 2–5 min, and reactions were started by mixing enzyme with substrate. Reaction volumes were usually 10–20 μL; reactions of over 1-h duration were performed in sealed microcapillary tubes to prevent evaporation. Reactions were quenched in 5 vol of 10 M urea/10 mM EDTA at 60 °C or by dilution into 20 vol of 0.1 M NaOAc/10 mM EDTA in ethanol in a dry ice/ethanol bath.

For assay of RNase P by cleavage of uniformly labeled pre-tRNA^{Asp} substrate, reaction mixes were electrophoresed in an 8% polyacrylamide/7 M urea/TBE gel to resolve pre-tRNA from mature tRNA and the 5′-leader sequence (Smith et al., 1991). For assay of cleavage of the 5′-end-labeled dA-, rA-, or rAm-tRNA substrates, the cleaved mononucleotide leader was resolved from precursor tRNA by ascending thin-layer chromatography on PEI cellulose in 1.2 M LiCl/1.2% boric acid. The excess salt from the reaction buffers was removed by preelutions in methanol followed by distilled water. Alternatively, descending chromatography on Whatman 54 or 3MM paper in 50% ethanol/0.5 M ammonium acetate was carried out. This latter method was found to be less sensitive to smearing than PEI cellulose chromatography due to salt in reaction buffers. Autoradiograms of the fixed and dried gels or chromatograms were used as templates to cut out the appropriate RNA bands, and the relative amount of RNA in each band was determined by Cerenkov scintillation. Background levels in negative controls were typically less than 0.002 of the total in cross-linking experiments and less than 0.01 of the total in cleavage experiments. These control values were subtracted from the experimental values to determine the extent of conjugation or cleavage.

In conditions of enzyme excess, the pre-tRNA^{Asp} and rA-tRNA^{Phe} substrates could be cleaved to 97% completion. The reactions with pre-tRNA^{Asp} and rA-tRNA^{Phe} followed first-order kinetics for ≥3 half-lives. Cleavage of the dA-tRNA^{Phe} substrate exhibited first-order kinetics for ≥2 half-lives, although it was usually analyzed by the method of initial rates due to its slow cleavage. Apparent first-order rate

constants were determined by the slope of the least-squares linear regression of a plot of ln (S_t/S_0) vs time, where S_0 is the initial amount of substrate and S_t is the amount of substrate remaining at a given time, equal to S_0 – product. Michaelian parameters were determined by a plot of $[S]/v$ vs [S] (the Hanes–Woolf plot), where [S] is the initial substrate concentration and v is reaction velocity. Standard deviations were calculated by assuming all of the error to be in the measurement of the velocity.

Because transcripts initiated with dinucleotide were not separated from those initiated with GTP, substrate preparations contained 10–20% mature tRNA as a contaminant. Mature tRNA is a competitive inhibitor of the RNase P reaction, with K_i approximately equal to K_M for pre-tRNA (Smith et al., 1992). Therefore, the mature tRNA will reduce both k_{cat} and K_M equally and in proportion to its fraction of the total substrate pool. No correction was made for this effect.

V_{max} determinations of cooperative reactions were estimated from the y-intercept of the least-squares exponential regression of a plot of $1/v$ vs $1/[Mg^{2+}]$. Because very slow reactions (large $1/v$) are given disproportionate weight by this method, data from reactions having less than one-fourth the rate of the fastest reaction were excluded.

RESULTS

Deoxy Substitution at the Cleavage Site. A pre-tRNA substrate that contains a unique deoxyribonucleotide substitution was constructed by using the dinucleotide dApG to "prime" in vitro transcription of a mature yeast $tRNA^{Phe}$ gene. We refer to this substrate as dA-$tRNA^{Phe}$ to indicate the addition of deoxyadenosine to the 5′-end of the tRNA. The effects of leader length and sequence were controlled by an unsubstituted substrate initiated with the dinucleotide rApG, referred to as rA-$tRNA^{Phe}$.

Both of these pre-tRNAs are substrates for RNase P RNA. Figure 1 is a thin-layer chromatogram of the products released from cleavage reactions. The substrates are 5′-end-labeled with ^{32}P, so that the expected products of cleavage are rAMP and dAMP. No dinucleotide product that would result from cleavage 3′ to the correct site was detected.

The steady-state kinetic parameters for rA-$tRNA^{Phe}$ cleavage are similar to those of more conventional pre-tRNAs having longer leader sequences (Table I). This result suggests that the pre-tRNA 5′-leader sequences have only minor effects on the enzyme–substrate interaction. Cleavage of the dA-$tRNA^{Phe}$ substrate is slow compared to its analog, rA-$tRNA^{Phe}$: k_{cat}/K_M is reduced 13-fold (Table I). This reduction can be attributed to k_{cat}; K_M is affected very little. Since K_M is approximately equal to K_d, the equilibrium dissociation constant (Smith et al., 1992), it appears that substrate binding is little affected by the deoxy substitution. The deoxy substrate has an increased Mg^{2+} requirement for cleavage (below). All results are reported for near-saturating levels of Mg^{2+} for each of the substrates: 25 mM for pre-$tRNA^{Asp}$ and rA-$tRNA^{Phe}$ and 100 mM for dA-$tRNA^{Phe}$. K_M for the deoxy-substituted substrate is not significantly different at 25 and 100 mM Mg^{2+} (not shown), as expected if Mg^{2+} primarily affects catalysis, rather than substrate binding.

The k_{cat} value reported in Table I for dA-tRNA is for a single turnover, meaning that the steps after the irreversible step (cleavage of the phosphodiester bond) cannot be rate-limiting.[1] Similar k_{cat} values are obtained for conditions of substrate excess or enzyme excess (not shown). At saturating levels of dA-$tRNA^{Phe}$, since only the single cleavage is measured, k_{cat} is expected to approach the rate of the cleavage step of the reaction, k_2. In contrast, the pre-$tRNA^{Asp}$ steady-state reaction is rate-limited by the release of product (Reich et al., 1988), so that its k_2 could be significantly faster than k_{cat}. The 30-fold reduction in k_{cat} for dA-$tRNA^{Phe}$ compared to rA-$tRNA^{Phe}$ therefore represents the minimal effect on the rate of the chemical step of the reaction.

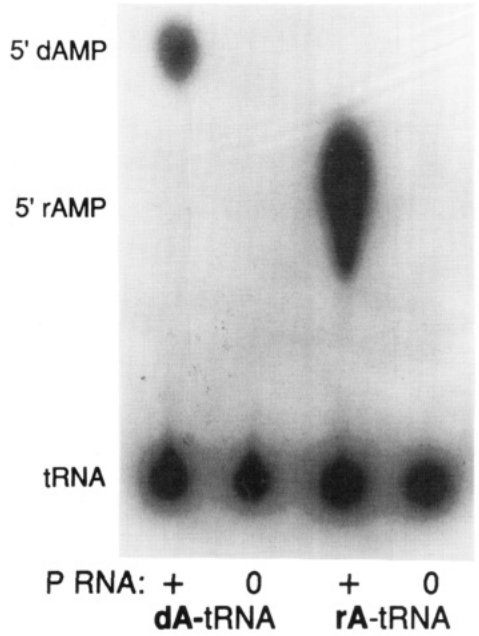

FIGURE 1: Release of the 5′-nucleotide by *E. coli* RNase P RNA in the dA- and rA-$tRNA^{Phe}$ reactions. Samples were spotted onto PEI cellulose thin-layer plates and developed by ascending chromatography in 1.2 M LiCl/1.2% boric acid. Radioactive spots were identified by their comigration with 5′-dAMP and 5′-AMP standards visualized by UV shadowing. pdApG, the product expected if the 5′-most ribose linkage in dA-$tRNA^{Phe}$ were cleaved, migrates halfway between 5′-rAMP and the origin.

OH^- Dependence of the Cleavage Reaction. We used a scheme based on the pH dependence of the cleavage reaction to estimate k_2, the rate of the catalytic step, for the ribo substrate. Previous reports on the influence of pH on the steady-state RNase P reaction found only a weak effect on cleavage rate (Marsh & Pace, 1985; Guerrier-Takada et al., 1986). However, the limitation of the steady-state reaction by release of product, not the catalytic step (Reich et al., 1988), compromises the interpretation of those results in terms of chemical mechanism.

We undertook to determine the rate of the catalytic step of the RNase P reaction with the possibility that catalysis might be slow and rate-limiting at low pH. Because the RNase P reaction is a hydrolysis, the mechanism may be written as

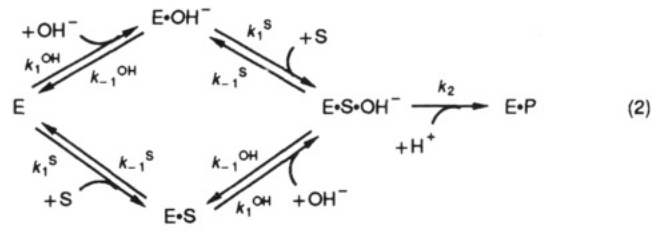

(2)

This mechanism is analogous to that of the *Tetrahymena* IVS ribozyme cleavage/transesterification reaction (Hershlag & Cech, 1991), in that OH^- is the nucleophile in place of

[1] Because the reactions are quenched by denaturation, both the free and enzyme-bound products are detected.

Table I: Kinetic Parameters of Cleavage Reactions

substrate[c]	cations	steady state k_{cat}, min^{-1}	steady state K_m, nM	pre-steady state k_2, min^{-1}	pre-steady state K_M^{OH}, μM
pre-tRNA^{Asp}	Na^+, Mg^{2+}	1.7 ± 0.05	130 ± 4.2	190 ± 8.4[a]	(4.1)[b]
pre-tRNA^{Asp}	Na^+, Ca^{2+}	nd	nd	0.013 ± 0.002[a]	4.1 ± 0.5
pre-tRNA^{Asp}	NH_4^+, Ca^{2+}	0.052 ± 0.006	21 ± 1.3	nd	nd
pre-tRNA^{Phe}	NH_4^+, Mg^{2+}	0.40 ± 0.01	48 ± 1.3	nd	nd
rA-tRNA^{Phe}	NH_4^+, Mg^{2+}	0.15 ± 0.02	62 ± 4.7	nd	nd
dA-tRNA^{Phe}	NH_4^+, Mg^{2+}	5.3×10^{-3} $\pm 3.2 \times 10^{-4}$	30 ± 7.4	nd	nd
dA-tRNA^{Phe}	Na^+, Mg^{2+}	0.074 ± 0.003	180 ± 10	0.056 ± 0.002[a]	1.7 ± 0.05
dA-tRNA^{Phe}	Na^+, Ca^{2+}	nd	nd	1.7×10^{-4} $\pm 2 \times 10^{-5}$ [a]	1.1 ± 0.2
rAm-tRNA^{Phe}	NH_4^+, Mg^{2+}	7×10^{-5}	nd	nd	nd

[a] Extrapolation to pH 8.0 from k_{cat} at pH 6.0 (see the Appendix). [b] Estimate from the Ca^{2+} reaction. nd, not determined. [c] Reaction conditions: pre-tRNA^{Asp} (Na^+, Mg^{2+}, steady state) = 0.5 nM *E. coli* RNase P RNA, 10–600 nM pre-tRNA^{Asp} in eight increments, 1.0 M NaCl, 25 mM $MgCl_2$, 25 mM HEPES, pH 8.0, 0.025% NP-40, 0.05% SDS; pre-tRNA^{Asp} (Na^+, Mg^{2+}, pre-steady state), see Figure 4 legend; pre-tRNA^{Asp} (Na^+, Ca^{2+}, pre-steady state), see Figure 2 legend; pre-tRNA^{Asp} (NH_4^+, Ca^{2+}), and pre-tRNA^{Phe} (NH_4^+, Mg^{2+}, from Smith et al. (1992); rA-tRNA^{Phe} (NH_4^+, Mg^{2+}) = 1.0 nM *E. coli* RNase P RNA, 20–400 nM rA-tRNA^{Phe} in six increments, 0.6 M NH_4Cl, 25 mM $MgCl_2$, 50 mM HEPES, pH 8.0, 0.05% NP-40, 0.05% SDS; dA-tRNA^{Phe} (NH_4^+, Mg^{2+}) = 200 nM *E. coli* RNase P RNA, 3–100 nM dA-tRNA^{Phe} in six increments, 0.6 M NH_4Cl, 25 mM $MgCl_2$, 50 mM HEPES, pH 8.0, 0.05% NP-40, 0.05% SDS; dA-tRNA^{Phe} (Na^+, Mg^{2+}, steady state) = 25–500 nM *E. coli* Rnase P RNA in five increments, 25 nM dA-tRNA^{Phe}, 1.0 M NaCl, 100 mM $MgCl_2$, 50 mM HEPES, pH 8.0, 0.05% NP-40; dA-tRNA^{Phe} (Na^+, Mg^{2+}, pre-steady state) and dA-tRNA^{Phe} (Na^+, Ca^{2+}, pre-steady state), see Figure 2 legend; rAm-tRNA^{Phe}, see Figure 5 legend.

Table II: Divalent Cation Cooperativity in Substrate Cleavage and Substrate Binding[e]

substrate	cation	Hill coefficient[a]	M^{2+} binding, K_d^{app} [b]
		Cleavage[c]	
pre-tRNA^{Asp}	Mg^{2+}	3.0 ± 0.2	8.9×10^{-7}
rA-tRNA^{Phe} (k_{cat}/K_M)	Mg^{2+}	3.1 ± 0.2	3.8×10^{-6}
rA-tRNA^{Phe} (k_2)	Mg^{2+}	3.2 ± 0.4	5.5×10^{-6}
dA-tRNA^{Phe}	Mg^{2+}	2.0 ± 0.1	6.4×10^{-3}
pre-tRNA^{Asp}	Ca^{2+}	1.5 ± 0.4	4.5×10^{-3}
tA-tRNA$_{Phe}$	Ca^{2+}	1.4 ± 0.2	1.0×10^{-3}
dA-tRNA^{Phe}	Ca^{2+}	1.0 ± 0.2	8.2×10^{-2}
		Substrate Binding[d]	
APA-tRNA^{Phe}	Mg^{2+}	1.0 ± 0.2	4.0×10^{-3}
APA-tRNA^{Phe}	Ca^{2+}	1.2 ± 0.4	3.2×10^{-3}

[a] From the slope of the Hill plot, log $v/V_{max} - v$ vs log $[M^{2+}]$. [b] Calculated from the Hill plot parameters $(y_{int}/slope)^{slope}$ (Segel, 1975). [c] Cleavage reaction conditions: pre-tRNA^{Asp} (Mg^{2+}) = 100 nM *E. coli* RNase P RNA, 10 nM pre-tRNA^{Asp}, 1–25 mM $MgCl_2$ in seven increments, 1.0 M NH_4Cl, 50 mM HEPES, pH 8.0, 0.05% NP-40; rA-tRNA^{Phe} (Mg^{2+}) and dA-tRNA^{Phe} (Mg^{2+}), see Figure 6 legend; pre-tRNA^{Asp} (Ca^{2+}) = 0.4 nM *E. coli* RNase P RNA, 5 nM pre-tRNA^{Asp}, 2–50 mM $CaCl_2$ in six increments, 1.0 M NH_4Cl, 50 mM HEPES, pH 8.0, 0.05% NP-40; rAhtRNA^{Phe} (Ca^{2+}), see Figure 6 legend; dA-tRNA^{Phe} (Ca^{2+}) = 100 nM *E. coli* RNase P RNA, 10 nM dA-tRNA^{Phe}, 25–250 mM $CaCl_2$, 1.0 M NH_4Cl, 50 mM HEPES, pH 8.0, 0.05% NP-40. [d] Cross-linking reaction conditions: APA-tRNA^{Phe} (Mg^{2+}), see Figure 6 legend; APA-tRNA^{Phe} (Ca^{2+}) = 50 nM *E. coli* RNase P RNA, 50 nM APA-tRNA^{Phe}, 0–50 mM $CaCl_2$ in seven increments, 1.0 M NH_4Cl, 50 mM HEPES, pH 8.0, 0.05% NP-40. [e] All results are from two or more independent experiments.

guanosine. The mechanism predicts the OH^- will behave as a simple Michaelian substrate when $[E] \gg K_S$ (the dissociation constant for the E·S complex), so that all of the substrate is bound to the enzyme, reducing the reaction to

$$E{\cdot}S + OH^- \underset{k_{-1}^{OH}}{\overset{k_1^{OH}}{\rightleftharpoons}} E{\cdot}S{\cdot}OH^- \xrightarrow[+H^+]{k_2} E{\cdot}P \qquad (3)$$

Because the ribo cleavage reaction in the presence of Mg^{2+} proved to be too fast to measure by manual methods, we used slower reactions to measure the rate dependence of k_2 on $[OH^-]$: cleavage in the presence of Ca^{2+} and cleavage of the dA-tRNA^{Phe} substrate in the presence of Ca^{2+} or Mg^{2+} (Table II). Figure 2 shows the rate dependence of these reactions under conditions of saturating enzyme and increasing $(OH^-]$. In all three cases, the dependence is hyperbolic.

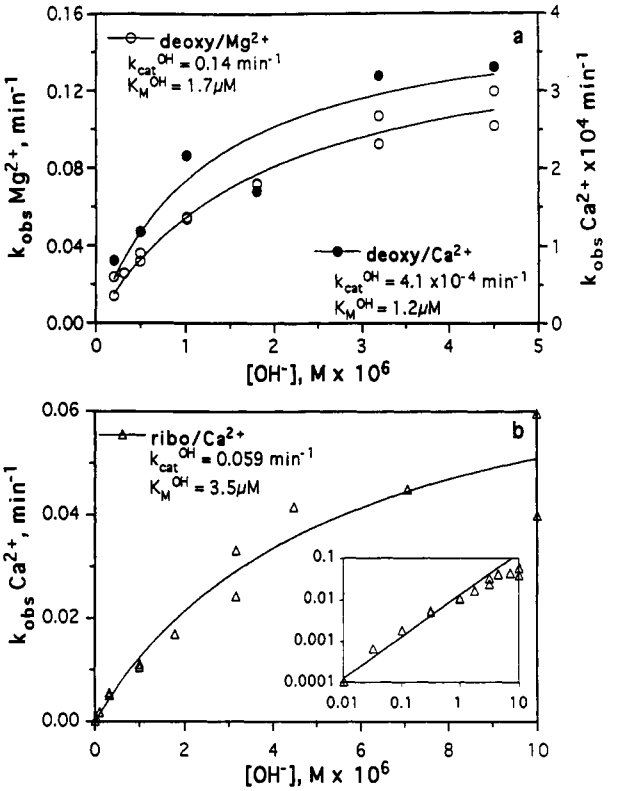

FIGURE 2: Dependence of cleavage rate on $[OH^-]$ at $[S] \gg K_S$. $[OH^-]$ is calculated as $10^{(pH-14)}$ M. Hyperbolic lines indicate the fit to the kinetic parameters shown. The insert in b is a log–log plot of the data, with the least-squares line drawn for $[OH^-] < 10^{-6}$ M. Reaction conditions: deoxy/Mg^{2+} = 500 nM *E. coli* RNase P RNA, 10 nM dA-tRNA^{Phe}, PT buffer (see Materials and Methods) at pH 6.00–8.65 in 11 increments, 1.0 M NaCl, 100 mM $MgCl_2$, 0.05% NP-40; deoxy/Ca^{2+} = 500 nM *E. coli* RNase P RNA, 25 nM dA-tRNA^{Phe}, PT buffer at pH 7.30–8.65 in six increments, 1.0 M NaCl, 200 mM $CaCl_2$, 0.05% NP-40; ribo/Ca^{2+} = 500 nM *E. coli* RNase P RNA, 50 nM pre-tRNA^{Asp}, PT buffer at pH 6.00–9.00 in 10 increments, 1.0 M NaCl, 50 mM $CaCl_2$, 0.05% NP-40.

One trivial explanation of the curves for rate vs $[OH^-]$ is that the ribozyme denatures at high pH, and the hyperbolae result from the combined effects of a first-order dependence upon $[OH^-]$ and RNA denaturation. The cross-linking reaction between 5′-azidophenacyl-tRNA and RNase P RNA provides a cleavage-independent assay of substrate binding

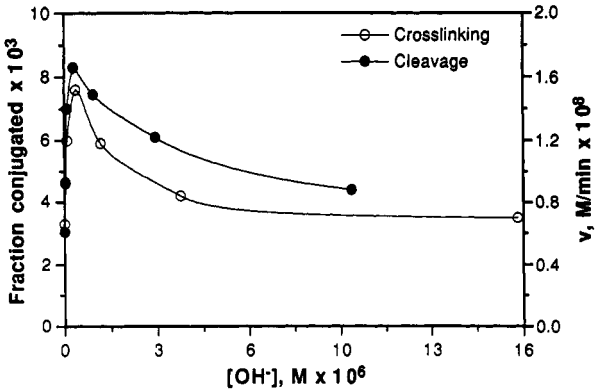

FIGURE 3: Dependence of substrate binding on [OH⁻]. Cleavage reactions are for a single turnover at [S] < K_M, where substrate binding is expected to be rate-limiting [K_M for a single turnover = $(k_1 + k_2)/k_1$ for scheme 1, was measured to be 0.4 μM at pH 6 (see Figure 4), and is expected to increase as k_2 increases with pH]. Reaction conditions: 20 nM *E. coli* RNase P RNA, 200 nM pre-tRNA^{Asp}, 1.0 M NaCl, 25 mM $MgCl_2$, PTD buffer (Materials and Methods) pH 6.0–9.0, at seven increments, 0.05% NP-40. Crosslinking reactions were under the same buffer conditions with 50 nM *E. coli* RNase P RNA, 50 nM APA-tRNA^{Phe}, 24 °C.

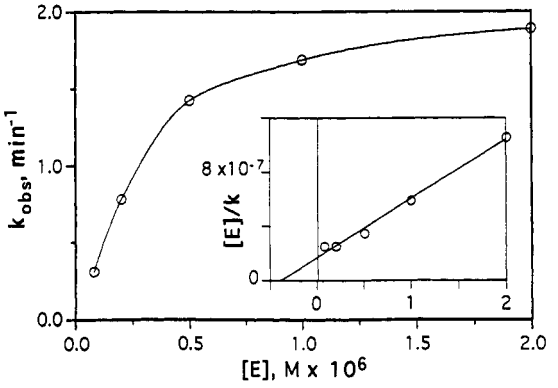

FIGURE 4: k_{cat} at pH 6.0. The inset shows the data as a Hanes–Woolf plot with the least-squares line from which k_{cat}^{pH6} was determined. Reaction conditions were *E. coli* RNase P RNA as indicated, 20 nM pre-tRNA^{Asp}, 1.0 M NaCl, 25 mM $MgCl_2$, Pt buffer, pH 6.0 (Materials and Methods), and 0.05% NP-40.

(Smith et al., 1992) and, hence, of the integrity of ribozyme and substrate structure (Figure 3). Also shown are pH effects on cleavage rates under k_{cat}/K_M conditions ([S] ≪ K_M), where substrate binding is expected to be rate-limiting. The effects of pH in these assays are similar and relatively weak, 2–3-fold per 10-fold change in [OH⁻] below pH 8.0. Above pH 8.0 ([OH⁻] ≥ 10^{-6} M), the effect on binding is even less. Because [E] = (5–10)K_M for the cleavage data in Figure 2, these small differences in apparent binding affinity are far too insufficient to account for the apparent saturation of rate with respect to [OH⁻].

The important conclusions from these experiments are the following: (1) k_2, the rate of the E·S → E·P conversion, is dependent on [OH⁻]; (2) the dependence is hyperbolic; and (3) the apparent Michaelis constant for OH⁻ (K_M^{OH}) is not significantly different for the deoxy reaction in the presence of Mg^{2+} or Ca^{2+} (Table II). Since the divalent cation does not affect K_M^{OH} for the deoxy cleavage reaction, it is reasonable to expect that K_M^{OH} for the ribo cleavage reaction in the presence of Mg^{2+} is similar to that of Ca^{2+}, about 4 μM.

The value for k_2 at pH 8.0 can be extrapolated from k_{cat} of the single turnover reaction at pH 6.0 (Figure 4). Because [OH]⁻ at pH 8.0 (1 μM) is less than K_M^{OH} (4 μM), the dependence of the rate on [OH⁻] is essentially first-order

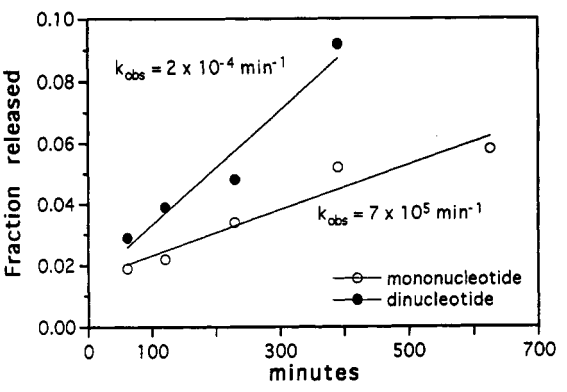

FIGURE 5: Cleavage of the 2′-*O*-methyl-substituted substrate. Positions of the mono- and dinucleotides were identified by comigration with unlabeled standards. Reaction conditions were 400 nM *E. coli* RNase P RNA, 100 nM rAm-tRNA^{Phe}, 1.0 M NH_4Cl, 50 mM $MgCl_2$, 50 mM HEPES, pH 8.0, and 0.05% NP40. Samples were spotted on Whatman 54 paper and resolved by descending chromatography in 50% EtOH/0.5 M NH_4OAc.

throughout the range pH 6–8. Application of the 100-fold increase in [OH⁻] from pH 6.0 to pH 8.0 to k_{cat}^{pH6} = 2.3 (± 0.1) min^{-1} gives a k_2 value at pH 8.0 of 230 (±9.7) min^{-1}. Application of the hyperbolic form of pH dependence (Appendix) gives k_2 = 190 (±8.4) min^{-1}.

Reduction of Reactivity by C2′ Substitutions. Comparison of k_2 values for the ribo and deoxy cleavage reactions allows estimation of the contribution of the 2′-OH group to reactivity. Deoxy substitution causes a catalytic rate (k_2) reduction of 3400-fold (Table I), compared to the ~30-fold effect indicated by comparison of steady-state k_{cat} values. The magnitude of this effect on k_2 suggests that the 2′-OH directly participates in the reaction. This participation plausibly involves the proton donor and/or acceptor functions of the 2′-OH. We tried to resolve these functions by evaluating the effects of a 2′-*O*-methyl substitution, which will retain acceptor, but not donor, function. This substrate was constructed in a fashion analogous to the dA-tRNA^{Phe} and rA-tRNA^{Phe} substrates by "priming" in vitro transcription with the dinucleotide rAmpG.

Cleavage of the 2′-*O*-methyl-substituted substrate is barely detectable. From the time course of cleavage at high concentrations of RNase P RNA (Figure 5), we estimate a catalytic rate on the order of 10^{-4} min^{-1}. This rate is extremely slow with respect to that of the ribo substrate and is significantly lower (>100-fold) than the rate for cleavage of the deoxy substrate. This result is consistent with a requirement for the 2′-OH proton and indicates a further defect, perhaps steric, imposed by the methyl group.

Accuracy of Cleavage Site Selection. Unlike the reactions of RNase P RNA with the rA-tRNA and dA-tRNA substrates, the mononucleotide resulting from cleavage at the expected site is not the unique product of the rAm-tRNA cleavage reaction. A dinucleotide corresponding to cleavage one nucleotide 3′ to the expected site is also detected. The rate of cleavage at this aberrant site is ~10^{-4} min^{-1}, which is 10^6-fold lower than the rate of cleavage of the rA-tRNA substrate at the proper site.

Catalysis Is Cooperatively Dependent on [Mg^{2+}]. Guerrier-Takada et al. (1986) reported a sigmoidal dependence of the RNase P RNA cleavage rate on [Mg^{2+}]. We repeated this observation under single turnover k_{cat}/K_M conditions; these data are presented in linear form (the Hill plot) in Figure 6a. Below 25 mM Mg^{2+}, the plot has a slope of 3.1 ± 0.2; the slope has an inflection and approaches 1 at [Mg^{2+}] > 25 mM. This inflection may signify a change in the rate-limiting step, possibly from catalysis to substrate binding, at higher [Mg^{2+}].

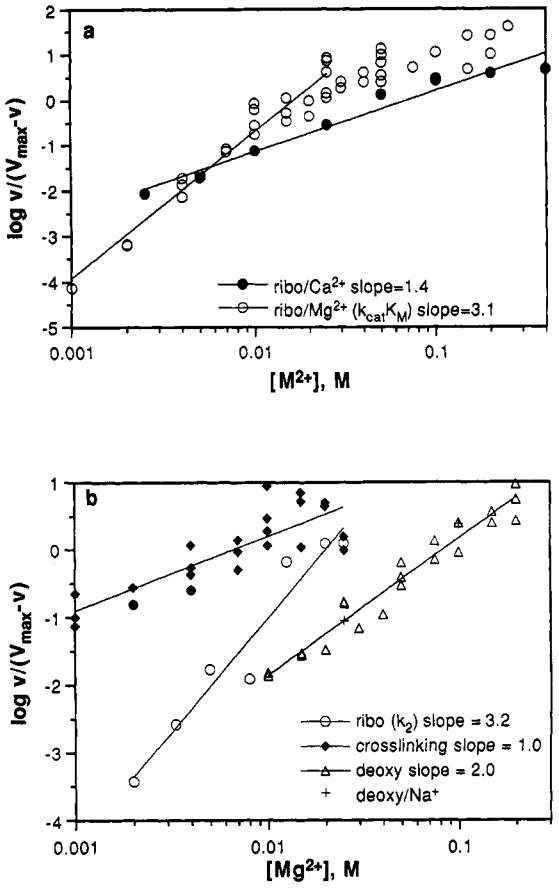

FIGURE 6: (a) Comparison of Mg^{2+} and Ca^{2+} cooperativity in the cleavage reaction. The least-squares line for the Mg^{2+} reaction is for $[Mg^{2+}] \leq 25$ mM. Reaction conditions: 100 nM *E. coli* RNase P RNA, 100 nM rA-tRNA^{Phe}, 1.0 M NH_4Cl, $MgCl_2$ or $CaCl_2$ as indicated, 50 mM HEPES, pH 8.0, 0.5% NP-40. (b) Resolution of Mg^{2+} cooperativity in catalysis and substrate binding and effect of deoxy substitution. Reaction conditions: cross-linking = 40 nM *E. coli* RNase P RNA, 40 nM APA-tRNA^{Phe}, $MgCl_2$ as indicated, 1.0 M NH_4Cl, 50 mM HEPES, pH 8.0, 0.05% NP-40. k_2 values for ribo cleavage were made by determining k_{cat}^{pH6} at each of the indicated $[Mg^{2+}]$; *E. coli* RNase P RNA was used in six increments from 0.2 to 2.0 μM, 50 nM pre-tRNA^{Asp}, 1.0 M NaCl, PTD buffer, pH 6.0, 0.05% NP-40. Deoxy cleavage for the points shown as triangles was at 20 nM *E. coli* RNase P RNA, 20 nM dA-tRNA^{Phe}, 1.0 M NH_4Cl, $MgCl_2$ as indicated, 50 mM HEPES, pH 8.0, 0.05% NP-40. For the points shown as crosses, the results are V_{max}^{app} determinations with 15–400 nM *E. coli* RNase P RNA in six increments, 20 nM dA-tRNA^{Phe}, 1.0 M NaCl, 25 or 100 mM $MgCl_2$, 50 mM HEPES, pH 8.0, 0.05% NP-40.

We used two approaches to distinguish cooperative effects on rate due to substrate binding from those due to catalysis. First, the $[Mg^{2+}]$ dependence on cross-linking extent was determined (Figure 6b, diamonds). The slope of the Hill plot for this assay of substrate binding was 1.0 ± 0.2, indicating that substrate binding is not cooperatively dependent on $[Mg^{2+}]$ and so could not account for cooperativity in the cleavage reaction. Second, we determined the effect of $[Mg^{2+}]$ on k_2 by the scheme described above: k_{cat}^{pH6} was determined at each of the Mg^{2+} concentrations represented by an open circle in Figure 6b (the primary data showing the dependence of velocity on [E] are not shown). The slope of the Hill plot for k_2 vs $[Mg^{2+}]$ determined in this manner is 3.2 ± 0.4, which is not significantly different from that of k_{cat}/K_M at low $[Mg^{2+}]$ (3.1 ± 0.2). For each of the Mg^{2+} concentrations of Figure 6b, the plot of velocity vs [E] is hyperbolic and not sigmoidal: there is no evidence for cooperative formation of enzyme multimers. We conclude that the catalytic step of the cleavage reaction has a strong cooperative dependence on $[Mg^{2+}]$.

The slope of the Hill plot of these data indicates that at least three Mg^{2+} ions are required for catalysis. This slope equals the number of ligands if cooperativity is high (the two-state model, in which all sites are simultaneously filled or empty) or gives the minimal number of ligands if intermediate numbers of sites are filled.

Cation Selectivity. We previously reported that Ca^{2+} is able to support the RNase P reaction at a reduced rate (Smith et al., 1992). Figure 6a shows that the catalytic rate has only a weakly cooperative dependence on $[Ca^{2+}]$, with a Hill coefficient of 1.4 ± 0.1. Concomitant with the loss in cooperativity, Ca^{2+} is weakly bound with an apparent dissociation constant of 0.02 M. Ca^{2+} is not a poor cofactor for the RNase P reaction solely because of its weak binding, as it reduces k_2 10^4-fold from the Mg^{2+}-catalyzed reaction even at saturation (Table I). In contrast to the effects on catalysis, Ca^{2+} is as effective as Mg^{2+} in promoting substrate binding (Smith et al., 1992; Table II).

The Substrate 2'-OH Is a Mg^{2+} Ligand. The Hill plot of the deoxy substrate is displaced toward higher $[Mg^{2+}]$ and has a lesser slope (2.0 ± 0.1) than that of the unmodified substrates, pre-tRNA^{Asp} and rA-tRNA^{Phe}. The difference in slopes holds for a 50-fold range of overlapping relative enzyme activity (v/V_{max} 0.01–0.5). These results may indicate that the enzyme–substrate complex containing the deoxy-substituted substrate has weakened affinity for Mg^{2+} and cooperatively binds one less Mg^{2+} ligand. An alternative interpretation of the reduced slope is that the cooperativity of Mg^{2+} activation of rate has been reduced.

DISCUSSION

The study of the RNase P reaction mechanism has been limited by the inability to assign changes in the observed cleavage rate to the catalytic step of the reaction. Because the catalytic step, k_2, is fast compared to the off-rates of pre-tRNA and mature tRNA, it does not contribute to any of the usual steady-state parameters. Effects of experimental variables on steady-state rates thus cannot be unambiguously assigned to either binding or catalytic steps.

We used pre-steady-state kinetic analysis of the RNase P RNA reaction to evaluate the rate of the catalytic step, k_2. Cleavage of unmodified pre-tRNA in the presence of Mg^{2+} is too fast to measure by manual methods; thus we slowed the reaction by using low pH. In order to extrapolate to physiological pH, the pH dependences of three slow reactions (deoxy/Mg^{2+}, deoxy/Ca^{2+}, ribo/Ca^{2+}) were determined. In all three cases, the catalytic step shows a hyperbolic dependence on $[OH^-]$ with half-maximal rates achieved at 1–5 μM $[OH^-]$, equivalent to pH 8.1–8.7. Within the range pH 6.0–8.0, the dependence is nearly first-order. The similarity of these pH responses indicates that they reflect fundamental properties of the reaction mechanism. We believe it reasonable to extrapolate from the slow reactions to the fast, native (ribo/Mg^{2+}) reaction to estimate the catalytic rate at physiological pH.

The rate of k_2 at physiological pH 7.5 is 70 (±3.1) min^{-1}; at the commonly used experimental pH 8.0 it is 190 (±8.4) min^{-1}. These rates are much larger than k_{cat} at the steady state for RNase P RNA (1.7 min^{-1}, Table I) and RNase P holoenzyme (10 min^{-1}; Waugh et al., 1989). Rates for each of the steps of the reaction can be assigned using the findings that binding of the pre-tRNA substrate is equivalent to that of mature tRNA product (Smith et al., 1992) and that k_{cat} represents the product release step (Reich et al., 1988):

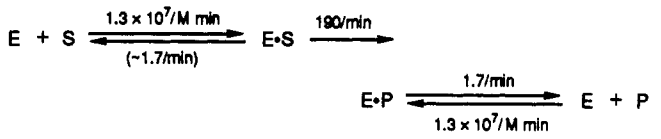

The net on-rate of $\sim 10^7$ M^{-1} min^{-1} is much less than that for a diffusion-controlled reaction (10^{10}–10^{11} M^{-1} min^{-1}) and also much less than that of aminoacyl-tRNA synthetases for tRNA ($\sim 10^{10}$ min^{-1}; Fersht, 1985). This rate is consistent with an intermediate step between initial binding of the substrate and formation of a catalytically active enzyme–substrate complex. On the basis of modification interference studies, Knap et al. (1990) have suggested that a partial unfolding of the tRNA acceptor helix occurs during binding.

pH and Mechanism. The hyperbolic dependence of k_2 on [OH^-] is used to calculate the rate of the catalytic step at physiological pH; this calculation is independent of the actual mechanism of pH dependence. Several mechanisms are consistent with the data. (1) OH^- could act as the nucleophile in the reaction and be treated as a Michaelian cosubstrate. This mechanism would be analogous to the *Tetrahymena* IVS cleavage reaction, and OH^- would fill the same role as guanosine. (2) Saturation with respect to [OH^-] could result from the titration of a general-base catalyst, which activates water for attack on phosphorus. The concentration of OH^- required for half-maximal rate, pH 8.0–8.5 (referred to as K_M^{OH} above), would then represent the pK_a of this base. The pK_a values of RNA functional groups closest to this range are for deprotonation of the N1 of uridine and the N3 of guanosine, at 9.5–10. (3) Apparent saturation could occur if first-order dependence on [OH^-] is combined with a deprotonation which inactivates catalysis without affecting substrate binding. The latter two models are less attractive than the first (OH^- is cosubstrate) on the teleological grounds that in the latter schemes a significant fraction of the enzyme would be inactive at physiological pH.

Accuracy of Cleavage. RNase P is remarkable in its specificity for cleavage at the correct substrate phosphodiester. Unlike the site of circle opening in the *Tetrahymena* IVS (Zaug & Cech, 1986), the RNase P cleavage site is not especially labile toward spontaneous hydrolysis (D. Smith, unpublished experiments), indicating that cleavage specificity arises primarily from enzyme–substrate binding interactions. We have been able to observe incorrect cleavage in only one instance: the reaction with the rAm-tRNA^{Phe} substrate, which yields measurable amounts of dinucleotide product resulting from cleavage 3′ to the correct bond. We estimate the second-order rate constant for this cleavage to be 2000 M^{-1} min^{-1},[2] which is equivalent to a 10^4-fold discrimination between adjacent phosphodiester linkages.

Divalent Cation Binding. The micromolar value of the apparent dissociation constant for Mg^{2+} indicates that a true binding site is formed by multiple contacts with the ribozyme. This binding site is remarkably specific. Ca^{2+} binds with an apparent dissociation constant on the order of 10^{-2} M, even though its affinity for nucleotide phosphates is similar to that of Mg^{2+} (Tu & Heller, 1974).

Although this tight binding of Mg^{2+} presumably results from multiple contacts with the ribozyme, these sites apparently are not required to stabilize the overall folding of the enzyme. The ribozyme can bind substrate in the absence of divalent cation; this binding implies that the ribozyme and substrate are essentially in native conformations. Mg^{2+} enhances substrate binding by ~10-fold, but it does so non-cooperatively and is no more effective than Ca^{2+}. The Mg^{2+}-binding sites detected through catalytic effects appear to be distinct and largely independent of those which affect structure. These properties are in contrast to those of the *Tetrahymena* IVS, which appears to be cooperatively dependent on Mg^{2+} for folding (Celander & Cech, 1990).

We have identified a possible ligand in one Mg^{2+}-binding site on the enzyme–substrate complex: the 2′-OH of the cleaved phosphodiester linkage. Removal of this 2′-OH by deoxy substitution reduces the Hill coefficient from 3 to 2 and increases the apparent Mg^{2+} dissociation constant from 16 μM to 6 mM. Ribose 2′-OH is not a good ligand for direct coordination to Mg^{2+}, but it can form an outer sphere complex by forming a hydrogen bond to a coordinated water.

The 2′-OH Group in Catalysis. A previous report on the effect of deoxy substitution at the substrate cleavage site (Forster & Altman, 1990) noted a ~40-fold decrease in cleavage rates; we found a similar effect under steady-state conditions (Table I). However, comparison of k_2 values for the ribo and deoxy cleavage reactions shows a much larger effect, 3400-fold at pH 8.0, indicating that this 2′-OH group is important for catalysis. These measurements were made at near-saturating levels of Mg^{2+}, so that the 3400-fold difference in rate is the effect on catalysis independent of metal-binding effects.[3] Much of this rate effect may be attributed to stabilization of the 3′-O^- leaving group by sharing of the 2′-OH proton. This effect, for example, reduces the pK_a of ribose relative to that of deoxyribose from ~15 to 12.4 (Izatt et al., 1965). The extremely slow rate of cleavage of the 2′-OMe-substituted substrate is consistent with a requirement for the 2′-OH proton.

It is possible that alterations in sugar conformation due to 2′ substitutions affect catalysis, but we believe that these effects are relatively minor. Although 2′-deoxyribose prefers the 2′-endo conformation, it can readily adopt the 3′-endo conformation of ribose (Saenger (1983), pp 61–62) and does so in mixed ribo/deoxyribo oligonucleotides (Egliet al., 1992). The 2′-*O*-methyl substitution forces the ribose into a C3′-endo conformation (Kawai et al., 1992).

Mg^{2+} and Catalysis. The involvement of Mg^{2+} in the reaction mechanism has been supposed because divalent cation can serve an RNA enzyme as a general acid in catalysis. On this bases, a mechanism for RNase P has been presented by Haydock and Allen (1985; Guerrier-Takada et al., 1986). This mechanism invokes a single Mg^{2+} ion, which ionizes water to form an OH^- nucleophile. The concomitant coordination of this Mg^{2+} with the substrate phosphate stabilizes the expected trigonal bipyramidal transition state. Our data, which show that at least three Mg^{2+} ions are involved in catalysis, indicate that this mechanism is at least incomplete. At least two additional Mg^{2+} ions must be accounted for in any explicit mechanism for RNase P action.

Additional roles for Mg^{2+} in a multiple Mg^{2+} reaction are suggested by the catalytic mechanism proposed for the *E. coli* DNA polymerase I exonuclease domain, which also has been proposed as a model for ribozyme-catalyzed phosphodiester cleavage (Freemont et al., 1988; Beese & Steitz, 1991). In this mechanism, deduced from the crystal structure, one Mg^{2+} promotes OH^- formation and a second acts to stabilize the

[2] Estimated by assuming that K_M is minimally perturbed by the 2′-*O*-Me substitution (~40 nM) and using $k_{cat} = 7 \times 10^{-5}$ min^{-1} from Table I: 7×10^{-5} $min^{-1}/4 \times 10^{-8}$ M = 1750 M^{-1} min^{-1}.

[3] We assume that Mg^{2+} binding is not precluded by the deoxy substitution, only weakened.

A. Pre-Transition State

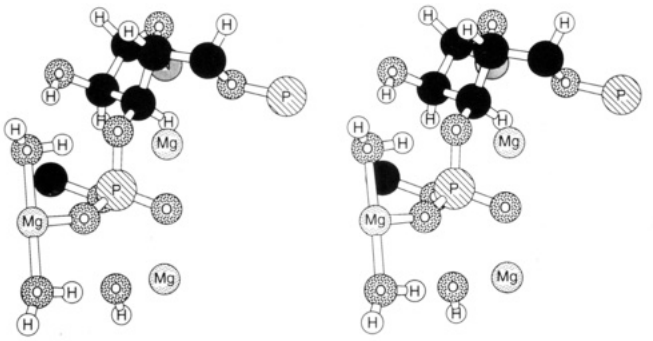

B. Reaction

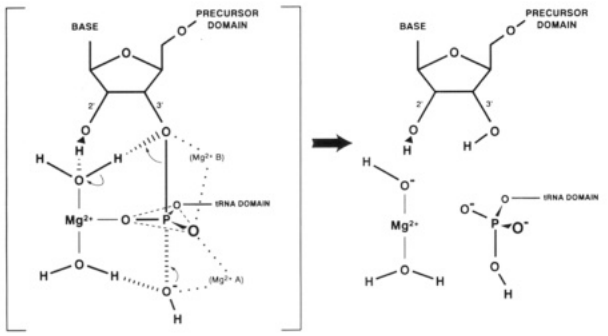

FIGURE 7: Possible mechanism for RNase P catalysis. (a) Cross-eyed stereo pair of the proposed complex. The phosphodiester backbone at the cleavage site is shown, running 5′ to 3′ from top left to bottom right. The backbone is in the RNA-A conformation, except that the 3′-OP bond has been rotated +30°. Covalent and coordination interactions are shown as cylindrical bonds; hydrogen bonds are stippled. The Mg^{2+} ion, on the left, coordinates through water to the 2′-OH group, accounting for the effect of 2′-deoxy substitution on Mg^{2+} cooperativity. The positions of the other two Mg^{2+} ions are from the model of Beese and Steitz (1991) and are included for comparison. All hydrogen-bonding distances are between 2.6 and 3.2 Å, and all coordination bonds are between 1.8 and 2.2 Å. (b) Proposed electron flow. Bold lines indicate covalent bonds. We assume the mechanism to be of the S_N2 in-line type. The attacking hydroxide is stabilized by hydrogen-bonding interactions with Mg-$(H_2O)_n$ and/or direct coordination with Mg^{2+}. This hydroxide may be formed through abstraction of H^+ by a coordinating Mg^{2+}-$(H_2O)_nOH^-$ complex, as proposed by Haydock and Allen (1985). The phosphorus moves into the plane of its oxygen atoms forming the trigonal bipyramidal transition state, which is stabilized by coordination to Mg^{2+}. The hydrogen-bonding interaction of the 2′-OH with water "steers" it into position to act as the proton donor to the 3′-O^- leaving group. The 2′-OH proton enhances reactivity by stabilizing the negative charge on the 3′-O^- and/or the donor water molecule. Substitution of this proton with a methyl group would displace this proton donor, accounting for the very poor reactivity of the 2′-*O*-methyl-substituted substrate.

transient negative charge on the 3′-O leaving group. Kinetic and spectroscopic analyses of the exonuclease reaction suggest, however, that a third metal ion, undetected by crystallography, is also important for catalysis (Han et al., 1991). There is also evidence for the involvement of three metal ions in the reaction mechanisms of P1 nuclease (Volbeda et al., 1991), alkaline phosphatase (Sowadski et al., 1985), and phospholipase C (Hough et al., 1989).

What we know of the RNase P reaction mechanism from previous work and this study can be summarized: (1) At least three Mg^{2+} ions participate in catalysis. (2) The 2′-OH group of the cleaved phosphodiester linkage appears to be involved in binding one of these Mg^{2+}. (3) Even at saturating concentrations of Mg^{2+}, the catalytic step for cleavage of a deoxyribose-substituted phosphodiester is reduced by a factor of 10^3–10^4. (4) Removal of the 2′-OH proton by substitution with a methyl group reduces the rate of catalysis much more than does simple deoxyribose substitution: $>10^5$-fold with respect to cleavage of a ribose linkage. This result indicates a requirement for the 2′-OH proton beyond charge stabilization of the 3′-O^- anion.

These observations indicate that the action of the RNase P mechanism involves the substrate 2′-OH. This conclusion is incorporated with the potential roles for Mg^{2+} discussed above into the stereochemical model depicted in Figure 7. In the model, the 2′-OH steers Mg^{2+} hydrate into coordination on the substrate phosphodiester. Because primary hydroxyls, including ribose 2′-OH, are known to be poor ligands for direct coordination to Mg^{2+}, we assume an outer sphere coordination through water. This complex can simultaneously coordinate directly to the substrate phosphate if a ca. +35° rotation from A-helix geometry about the C3′–O3′ bond is made. Because *E. coli* pre-tRNAs are generally unpaired or weakly (U–A or U–G) paired at this position, the disruption of base-pairing accompanying this rotation would not be strongly disfavored. Indeed, Knap et al. (1990) have reported some evidence of helix disruption in this region of the enzyme–substrate complex. A Mg^{2+} in this configuration is further able to coordinate, through water, to an OH^- positioned for in-line attack on the phosphorus. According to the model of Haydock and Allen (1985), the Mg^{2+} hydrate generates this nucleophilic OH^-.

Although this model accounts explicitly for only one of the catalytic Mg^{2+} ions, it does explain several features of the reaction. (1) It provides a highly constrained binding site for Mg^{2+}, consistent with the high degree of ion selectivity of the reaction. (2) By hydrogen bonding the water molecule which serves as the proton donor to the 2′-OH, the model explains the near inability of RNase P RNA to cleave at a 2′-OH-substituted linkage. Whereas deoxyribose substitution might abolish the steering of this water to the 3′-O, the bulk of the methyl group would sterically exclude the water. (3) The multiple contacts with the substrate phosphodiester linkage and the cosubstrate OH^- provide the potential for cooperativity, either in binding or in catalytic activation. If two or more Mg^{2+} ions coordinate in concert with a common ligand, the most stable binding and optimal transition-state geometry might not be attained until all ligands are in place.

ACKNOWLEDGMENT

We thank O. Uhlenbeck for helpful discussions on the interpretations of the pH curves.

APPENDIX

OH^- as Cosubstrate. Under conditions of low pH, that is, $[OH^-] \ll K_M^{OH}$, binding of OH^- will be rate-limiting for the cleavage reaction, and $k_2/K_M^{OH} = v/[E{\cdot}S][OH^-]$. The quantity $[E{\cdot}S] = [S]$ when all of the substrate is bound to enzyme, that is, when $v = V_{max}$ with respect to [E]. We therefore determined k_{cat}^{pH6} ($[OH^-] = 10^{-8}$ M, $\ll K_M^{OH}$) by measuring the reaction velocity in the presence of increasing [E], as shown in Figure 3. At saturating [E], $v = V_{max}$ $[E{\cdot}S] = [S]$, and $k_{cat}^{pH6} = V_{max}/[E{\cdot}S] = 2.3 \pm 0.1$ min^{-1}. Using $K_M^{OH} = 3.5$ μM, the rate of the breakdown of the E·S·OH^- complex to E·P equals

$$V_{max}/([E{\cdot}S][OH^-])K_M^{OH} = 940 \text{ min}^{-1} \qquad \text{(A1)}$$

which is k_2 at saturating (infinite) $[OH^-]$. The same value is obtained for a mechanism in which rate saturation results from titration of a general-base catalyst.

First-Order Dependence on [OH⁻] Coupled with a Deprotonation. For the reaction conditions used, where enzyme is excess of, and saturating with respect to, substrate,

$$k_{obsd} = k_{chem}[OH^-]E_A/E_T \quad (A2)$$

where k_{chem} is the rate of decomposition of the E·S·OH⁻ complex to E·P, E_A is the fraction of active enzyme, and E_T is the total enzyme. The quantity E_A/E_T can be evaluated using the Henderson–Hasselbach equation:

$$pH = pK_a + \log B/A \quad (A3)$$

where K_a is the equilibrium constant for the deprotonation event(s), B is the concentration of the basic, inactivated form of the enzyme ($= E_T - E_A$), and A is the concentration of the active enzyme. To solve in terms of [OH⁻], we use the identity, pH = log ([OH⁻]/10^{-14}), to give

$$\log \frac{[OH^-]}{10^{-14}} = -\log K_a + \log \frac{E_A - E_T}{E_A} \quad (A4)$$

$$\frac{E_A}{E_T} = \frac{1}{1 + \left\{\frac{K_a[OH^-]}{10^{-14}}\right\}} \quad (A5)$$

Substitution from eq A2 and rearrangement gives

$$k_{obsd} = \frac{k_{chem}}{(K_a/10^{-14}) + (1/[OH^-])} \quad (A6)$$

which is also hyperbolic in form. K_a and k_{chem} can be solved using a linear form of the equation:

$$\frac{[OH^-]}{k_{obsd}} = \frac{1}{k_{chem}} + \frac{K_a}{k_{chem}}\left(\frac{[OH^-]}{10^{-14}}\right) \quad (A7)$$

For the ribo/Mg^{2+} cleavage reaction at infinite [OH⁻], $k_{chem} = 2 \times 10^8$ min⁻¹.

REFERENCES

Altman, S. (1989) *Adv. Enzymol. Relat. Areas Mol. Biol. 62*, 1.

Beese, L. S., & Steitz, T. A. (1991) *EMBO J. 10*, 25.

Burgess, J. (1988) *Ions in Solution: Basic Principles of Chemical Interactions*, Ellis Horwood Ltd., Chichester, England.

Burgin, A. B., & Pace, N. R. (1990) *EMBO J. 9*, 4111.

Cech, T. R. (1987) *Science 236*, 1532.

Celander, D. W., & Cech, T. R. (1991) *Science 251*, 401.

Egli, M., Usman, N., Zhang, S. G., & Rich, A. (1992) *Proc. Natl. Acad. Sci. U.S.A. 89*, 534.

Ellis, K. J., & Morrison, J. F. (1982) *Methods Enzymol. 87*, 405.

Fersht, A. (1985) *Enzyme Structure and Mechanism*, 2nd ed., p 151, W. H. Freeman & Co., New York.

Forster, A. C., & Altman, S. (1990) *Science 249*, 783.

Freemont, P. S., Friedman, J. M., Beese, L. S., Sanderson, M. R., & Steitz, T. A. (1988) *Proc. Natl. Acad. Sci. U.S.A. 85*, 89243.

Guerrier-Takada, C., Haydock, K., Allen, L., & Altman, S. (1986) *Biochemistry 25*, 1509.

Han, H., Rifkind, J. M., & Mildvan, A. S. (1991) *Biochemistry 30*, 11104.

Haydock, K., & Allen, L. C. (1985) in *Progress in Clinical and Biological Research 172A*, pp 87–98, A. R. Liss, Inc., New York.

Hershlag, D., & Cech, T. R. (1990a) *Nature 344*, 405.

Hershlag, D., & Cech, T. R. (1990b) *Biochemistry 29*, 10159.

Hough, E., Hansen, L. K., Birknes, B., Jynge, K., Hansen, S., Hordvik, A., Little, C., Dodson, E., & Derewenda, Z. (1989) *Nature 338*, 357.

Izatt, R. M., Hansen, L. D., Rytting, J. H., Christensen, J. J. (1965) *J. Am. Chem. Soc. 87*, 2760.

Kawai, G., Yamamoto, Y., Kamimura, T., Masegi, T., Sekine, M., Hata, T., Iimori, T., Watanabe, T., Miyazawa, T., & Yokoyama, S. (1992) *Biochemistry 31*, 1040.

Knap, A. K., Wesolowski, D., & Altman, S. (1990) *Biochimie 72*, 779.

Marsh, T. L., & Pace, N. R. (1985) *Science 229*, 79.

Martin, C. T., & Coleman, J. E. (1989) *Biochemistry 28*, 2760.

Milligan, J. F., & Uhlenbeck, O. C. (1989) *Methods Enzymol. 180*, 51.

Pace, N. R., & Smith, D. (1990) *J. Biol. Chem. 265*, 3587.

Randerath, K., & Randerath, E. (1967) *Methods Enzymol. 12A*, 323.

Reich, C. I., Olsen, G. J., Pace, B., & Pace, N. R. (1988) *Science 239*, 178.

Saenger, W. (1984) *Principles of Nucleic Acid Structure*, pp 107–110, Springer-Verlag, New York.

Segel, I. H. (1975) *Enzyme Kinetics*, John Wiley & Sons, New York.

Smith, D., Burgin, A. B., Haas, E. S., & Pace, N. R. (1992) *J. Biol. Chem. 267*, 2429.

Sowadski, J. M., Handschmacher, M. D., Krishna Murthy, H. M., Foster, B. A., & Wyckoff, H. W. (1985). *J. Mol. Biol. 186*, 417.

Tu, A. T., & Heller, M. J. (1974) in *Metals Ions in Biological Systems Vol. 1, Simple Complexes*, (Sigel, H., Ed.) pp 2–45, Marcel Dekker, New York.

Volbeda, A., Lahm, A., Sakiyama, F., & Suck, D. (1991) *EMBO J. 10*, 1607.

Waugh, D. S., Green, C. J., & Pace, N. R. (1989) *Science 244*, 1569.

Zaug, A. J., Kent, J. R., & Cech, T. R. (1985) *Biochemistry 24*, 6211.